REPORT SERIES IN AEROSOL SCIENCE
N:o 149 (2014)

FRAGMENTATION AND BOUNCE OF NANOSIZE AGGLOMERATES BY INERTIAL IMPACTION

Mika Ihalainen

Faculty of Science and Forestry
University of Eastern Finland
Kuopio, Finland

Academic Dissertation

To be presented, with permission of the Faculty of Science and Forestry of the University of Eastern Finland, for public examination in Auditorium L21, Snellmania Building at the University of Eastern Finland, Kuopio, on 25th April, 2014, at noon.

Kuopio 2014

Author's address: Fine Particle and Aerosol Technology Laboratory
University of Eastern Finland
Department of Environmental Science
P.O.Box 1627
70211 Kuopio
Finland

Supervisors: Professor Jorma Jokiniemi, Ph.D.
University of Eastern Finland
Department of Environmental Science

Doctor Terttaliisa Lind, Ph.D.
Paul Scherrer Institut
Nuclear Energy and Safety Research Department
Villigen, Switzerland

Professor Kari Lehtinen, Ph.D.
University of Eastern Finland
Department of Applied Physics

Reviewers: Professor Kaarle Hämeri, Ph.D.
University of Helsinki
Department of Physics
Helsinki, Finland

Doctor Marko Marjamäki, Ph.D.
Fortum Oyj
Espoo, Finland

Opponent: Professor Wolfgang Koch, Ph.D.
Fraunhofer Institute for Toxicology and Experimental Medicine
Department of Aerosol Research and Analytical Chemistry
Hannover, Germany

ISBN 978-952-5822-90-8 (printed version)
ISSN 0784-3496
Helsinki 2014
Unigrafia Oy

ISBN 978-952-5822-91-5 (PDF version)
http://www.atm.helsinki.fi/FAAR/
Helsinki 2014

Mika Marko Tapio Ihalainen,
University of Eastern Finland, 2014

Abstract

In this thesis, the inertial impaction of nanosize agglomerates was investigated. The study focused on two processes that occur commonly simultaneously during the impaction of the agglomerate; bounce and fragmentation. The main objective was to study how different parameters affected these processes. The parameters that were considered included the impaction velocity, agglomerate properties, such as the composition and primary particle size, and impaction surface material.

A measurement system to study the impaction of an agglomerate was designed. It included a size classifier, a multi-orifice impactor, and a custom low-pressure sampling chamber which was utilized for the collection of the bounced particles. The fragmentation was defined by comparing the size of the agglomerates before and after the impaction. The mass balance before and after the impaction was also estimated to find out the fraction of the bounced particles.

The agglomerate properties had an effect on their impaction behavior. For example, the bounced fraction decreased but the fragment size did not change notably as the primary particle size was decreased. Enhanced degree of sintering increased the fragment size due to stronger bonds between the primary particles. At the lowest impaction velocity, a considerable fraction of the agglomerates bounced without fragmentation at the lowest impaction velocity in most cases.

An important observation was that the bounce fraction did not increase with the increasing impaction velocity in every case. This was probably due to increased adhesion between the agglomerate and the surface that arises from the fragmentation. In addition, the fragmentation process reduces the energy available for the bounce.

The effect of metallic impaction plate materials was little on either the fragmentation or the bounce at the velocities used in this study.

Keywords: Fragmentation, Bounce, Inertial impaction, Agglomerate, Nanoparticle

Preface

This thesis would have not been possible without the co-operation of two groups, Laboratory for Thermal-Hydraulics at Paul Scherrer Institut and Fine Particle and Aerosol Technology Laboratory at the University of Eastern Finland. The studies were financially supported by ARTIST II program and the University of Eastern Finland provided the facilities.

I express my gratitude to my principal supervisor Prof. Jorma Jokiniemi for the guidance with the thesis and providing an excellent environment for scientific work. I wish to express my gratitude to my supervisor Dr. Terttaliisa Lind for all the help with this thesis. She guided me patiently with all the troubles I ran into with the thesis. I am also grateful to Prof. Kari Lehtinen for his encouragement and supervision of this thesis.

I am grateful to my official reviewers Professor Kaarle Hämeri and Doctor Marko Marjamäki for valuable comments. I wish to thank Professor Wolfgang Koch for kindly accepting the invitation to serve as an opponent in the public examination of this dissertation.

I am thankful to all my co-authors and colleagues for the successful co-operation. Thank you present and former members of FINE for your support and friendship! It has been inspiring and 'very much' fun to work with you all. I am also grateful to people of the LTH at PSI who treated me with kindness and supported me in my work.

I thank my family for supporting me and being there for me. Finally, thank you Pia for your love and understanding. Thank you for reminding me that the work is only a part of the life.

List of publications

This thesis consists of an introduction to the subject and results followed by four research papers

Paper I Ihalainen, M., Lind, T., Torvela, T., Lehtinen, K. E. J. & Jokiniemi, J. (2012) A Method to Study Agglomerate Breakup and Bounce During Impaction. *Aerosol Science and Technology*. 46: 9, 990-1001.

Paper II Ihalainen, M., Lind, T., Arffman, A., Torvela, T. and Jokiniemi, J. (2014) Break-Up and Bounce of TiO_2 Agglomerates by Impaction. *Aerosol Science and Technology*. 48:1, 31-41.

Paper III Ihalainen M., Lind T., Ruusunen, J., Tiitta, P., Lähde A., Torvela T. and Jokiniemi J. Bounce of submicron agglomerates during inertial impaction. Submitted to *Powder Technology*.

Paper IV Ruusunen, J., Ihalainen, M., Koponen, T., Torvela, T., Tenho, M., Salonen, J., Sippula, O., Joutsensaari, J., Jokiniemi, J. and Lähde, A. (2014) Controlled oxidation of iron nanoparticles in chemical vapour synthesis. *Journal of Nanoparticle Research*. 16:2270

Contents

1 INTRODUCTION

Agglomerates are described as a set of primary particles that are connected to each other at random locations, forming a chainlike structure with many branches. Now, let us put a solid wall nearby and give the agglomerate a velocity toward the wall. Eventually, it will impact the wall, and during the impaction, the agglomerate will undergo forces that twist and bend it. If the magnitudes of these forces are sufficiently high, then the initial agglomerate is shattered to smaller blocks, which contain a seemingly random number of primary particles. Because there is also adhesion between the particles and the wall, a portion of the fragments may stay in contact with the wall, and a portion will bounce away from the wall. In this study, the agglomerate break-up and bounce, which are often coexisting processes, due to inertial impaction are investigated. The effects of agglomerate properties, such as primary particle size and material, in addition to the system parameters, such as the impaction target material, on the impaction process are investigated.

What happens to a particle during inertial impaction has been of concern in various areas of aerosol research. The bounce alone plays a significant role, for example, in aerosol collection methods that are based on inertial impaction, in which bounce suppression is desired (Dunbar et al., 2005; Lai et al., 2008; Cheng and Yeh, 1979 and Pak et al., 1992). The bounce, however, is not always an undesired phenomenon. Virtanen et al. (2010) used the bounce during inertial impaction to evaluate the physical state of the particle. In nuclear reactors, during Steam Generator Tube Rupture (SGTR) situations, the bounce, along with fragmentation, is also a subject of interest for Guntay et al. (2004). In those situations, inertial impactions, which take place near a tube breach, may affect the aerosol distribution and, hence, the transport properties of nuclear aerosols, which are an

important part of the source term, i.e., radioactive material release to the environment.

During the last decade, there has been progress in the experimental investigation of the fragmentation of nanosize, that is less than 1 μm in size, agglomerates during inertial impaction (Seipenbusch et al., 2002; Seipenbusch et al., 2007; Seipenbusch et al., 2010; Froeschke et al., 2003 and Rothenbacher et al., 2008). In these studies, a single stage low-pressure impactor with a single orifice has been used to impact the particles, and the Transmission Electron Microscope (TEM) micrographs before and after the impaction have been compared to determine how many interparticle bonds broke during impaction.

In their experiments, Seipenbusch et al. (2007) found that the minimum kinetic energy that was required to induce fragmentation of the agglomerate was dependent on the size of the primary particles in the agglomerate; the smaller the size of the primary particle was, the higher the minimum kinetic energy. Seipenbusch et al. (2007) also determined that the bonding energies of Ag agglomerates followed a theory that was based on the Weibull statistics (Weibull, 1951), as long as the Ag agglomerates were large enough (few hundred nanoparticles per agglomerate). However, the bonding energies of Pt agglomerates were one order of magnitude higher than the bonding energies that were predicted by the theory. It was hypothesized that this observation could be due to a possible sintering, that is formation of necks between the primary particles, of Pt agglomerates, which would strengthen the bonds between the primary particles. Instead, the Ag particles were far less prone to sintering because the Ag particles were more easily oxidized. With respect to Ni, these researchers noted that the relation of the minimum threshold energy for fragmentation to the primary particle size was not as linear as the minimum threshold energies for Ag and Pt. This result was explained by magnetic dipole attractive forces, which were established between Ni primary particles, which exceeded a critical size of approximately 12 nm. The dependence of the kinetic energy that was required to

induce fragmentation on primary particle size was also observed in the studies of Froeschke et al. (2003). Furthermore, Froeschke et al. (2003) determined that there was no fragmentation with Ni agglomerates, even at a velocity of 120 m/s. Possible reasons for this behavior include the following: relatively small primary particle size (4 nm), high fractal dimension (2.5), and the super paramagnetic behavior of Ni nanoparticles. The experimental fragmentation energies of Ag agglomerates were also compared with estimated bond energies, which were based on pure Van der Waals interactions, and found that the measured energies were approximately 5 times higher than the calculated values, when only Van der Waals interactions were assumed. The fragmentation of SiO_2 agglomerates that have different degrees of sintering was studied by Seipenbusch et al. (2010), who determined that because the primary particles were held together with a relatively weak force, the agglomerates were almost entirely fragmented to primary particles. However, by increasing the solid necking between the primary particles, fragmentation decreased until the agglomerates did not fragment.

For supermicron, larger than 1 μm in size, particles, the fragmentation that is due to inertial impaction has been studied experimentally. John and Sethi (1993) studied agglomerate break-up by impacting supermicron latex doublets and by measuring these doublets optically before and after the impaction. These researchers observed that the measured energy that was needed to break-up half of the doublets was over 3000 times higher than the theoretical energy that was estimated from the pure Van der Waals interface between the primary particles and concluded that this measured energy was most likely due to the formation of bridges between particles by residues that were left after droplet evaporation. Wong et al. (2011) studied the break-up of pharmaceutical agglomerates of several hundred micrometers upon impaction. These researchers found that the particle size after impaction was dependent on the air velocity that was directly above the impactor plate and not on the impaction velocity. Cheong et al. (2003) investigated the effect of the

impaction angle and velocity on millimeter glass spheres. These researchers found that the glass spheres experienced elastic behavior at low impaction velocities and shallow impaction angles, whereas plastic failure prevails at high impaction velocities and steep impaction angles, which led to fragmentation. Salman et al. (2002) also studied millimeter single particle impaction and found that, as the particle size increased, the maximum velocity at which no fragmentation occurred decreased. The thickness and materials of the impaction plate were also varied in their experiments, and these researchers concluded that both the plate material and thickness had a significant effect on the impaction outcome. Specifically, these researchers found that a thin or soft target reduced fragmentation.

Numerical methods have also been used investigate the fragmentation process of impacting supermicron agglomerates. The discrete element method (DEM) has been the tool of choice in most studies regarding fragmentation. The effect of impaction velocity and angle on the fragmentation has been studied, e.g., by Tong et al. (2009), Thornton et al. (1999), Moreno et al. (2003) and Wittel et al. (2008). Other parameters examined have been, for example, packing density (Mishra and Thornton, 2001), shape of the agglomerate (Liu et al., 2010) and how energy is dissipated during impaction (Moreno-Atanasio, 2012). The numerical investigations focused on spherical or close to spherical agglomerates, however, for nanosize open agglomerates, there have only been a few studies. Lechman (2010) and Lechman and Takoto (2010) applied the DEM method to study the fragmentation of an open nanosize agglomerate during an impaction with a rigid wall. Lechman and Takoto (2010) suggested that the probability of a given ejected cluster size followed a velocity power law with exponent 0.3.

In addition to the inertial impaction, the fragmentation of the agglomerates has been studied using other methods. For example, Wengeler et al. (2006), Wengeler and Nirschl (2007) and Teleki et al. (2008) used the dispersion of agglomerates through a nozzle at high pressure to fragment the agglomerates. Lind et al. (2010) studied the

effect of turbulent flows on fragmentation in the SGTR situation, and the ultrasonic fragmentation of agglomerates that are suspended in liquids have been investigated by, e.g., Kusters et al. (1993); Mandzy et al. (2005); Marković et al. (2008).

Until recently, research regarding the bounce of nanosize agglomerates has been restricted to applications, such as efforts to minimize bounce in impactors. However, Rennecke and Weber studied the bounce of nanosize particles during inertial impaction. These researchers found that the critical velocity to make the particle overcome the adhesive forces between the surface and the particle was in the same order of magnitude as that of larger supermicron particles. Previously, it was determined that, for particles over a micron, the critical velocity increases as the particle size decreases. The extrapolation to the nanosize particle size range would give an assumption that the required critical velocity for the bounce would be much higher than that found by Rennecke and Weber. Rennecke and Weber suggested that this difference could be due to the change in the deformation mode between the elastically deforming nanosize particles and micron particles, where plastic deformation is the main form of energy dissipation.

More extensive research has been performed regarding the parameter that affects supermicron particle bounce. Both normal (e.g., Wall et al., 1990; Dunn et al., 1995 and Li et al., 1999) and oblique (e.g., Dunn et al., 1995; Li et al., 1999; Konstandopoulos, 2006 and Li et al., 2000) impactions have been studied. In oblique impactions, the friction between the particle and surface affects the process, in addition to adhesion, which dominates the process in normal impactions Brach et al. (2000). These impaction studies have shown that the coefficient of restitution, that is the ratio of velocity after bounce to the initial velocity, decreases rapidly as the initial velocity decreases, whereas the initial velocity is close to the critical velocity where the capture occurs. Because the initial velocity is considerably higher than the critical velocity, the coefficient of restitution is only slightly sensitive to the initial velocity changes. Increasing the particle

size has been found to decrease the critical velocity that is required. Wall et al. (1990) found that the critical velocity has an explicit power-law dependence on the particle size. However, this type of dependency was not found for oblique impacts (Konstandopoulos, 2006). For oblique impacts, the tangential velocity is not thought to affect the normal process of impact; thus, the stick/bounce behavior should be affected by the normal velocity. However, Li et al. (2000) implied that the process of the capture of microparticles is more complex. Li et al. also showed that the capture is more likely for normal impacts than for oblique impacts.

Many studies have used numerical methods to cover different aspects that affect the particle bounce due to impaction with a flat surface. Work have been conducted for normal and oblique impacts in which the particle deformation has been considered as inelastic (Stronge et al., 2001), elastic (Jayadeep et al., 2013 and Thornton and Yin, 1991) or plastic (Wu et al., 2003; WU et al., 2008; Feng et al., 2009; Thornton et al., 2013; Weir and McGavin, 2008; Liu et al., 2011; Thornton and Ning, 1998 and TSAI et al., 1990). The commonly found bounce behavior for elastic particles is that the particles stick to the surface at low impaction velocities but start to bounce once the critical velocity is reached and the bounce probability increases as the impaction velocity is further increased (Thornton and Ning, 1998). For particles which may deform plastically the process is, however, more complicated. Jung et al. (2010) and Awasthi et al. (2007) showed more complicated bounce results with nanosize clusters with Lenard-Jones type bonding. At low velocities, the clusters progress from adhesion to bounce as the impaction velocity increases. However, as the velocity is further increased, the clusters plastically deform. This increases the adhesion between the cluster and the impaction surface which leads to the decreasing bounce probability with increasing impaction velocity. The bounce probability increases again as the impaction velocity is increased as the kinetic energy overcomes the increased adhesion at high impaction velocities. The bounce simulations have not been restricted to study only the properties of

the impacting particle. For example, Qin and Pletcher (2011) investigated the effect of surface asperity deformations on the particle impact. Abd-Elhady et al. (2006) simulated the interaction between a particle impacting a bed of particles and found that the maximum indentation in the bed was directly proportional to the incident particle velocity and diameter if plastic deformation occurred.

The traditional method to experimentally study fragmentation by inertial impaction is to compare the agglomerates or spheres before impaction to those agglomerates or spheres after impaction. For larger particles, methods that are based on visual observation are also available. For example, Kwek et al. (2013) used high-speed imaging to track the fragmentation process of supermicron spray-dried mannitol particles.

The evaluation of the impaction velocity of the nano agglomerates has been a profound problem in the study of inertial impaction. Although the first study to experimentally evaluate the impaction velocity was published by Reuter-Hack et al. (2007), there are no systematic measurements on this issue. Impaction velocity is a key factor because impaction velocity is strongly related to the initial kinetic energy that is available for the processes that take place during impaction. In earlier studies, the ratio of the impaction velocity to the gas jet velocity was estimated to be 0.85, which originated from the early study by Marple (1970). This method, however, has remained a controversial way to describe impaction velocity as a rule and was shown to overestimate the impaction velocity at lower jet velocities and to underestimate the impaction velocity at higher velocities, as demonstrated by Rennecke and Weber (2013). These researchers proposed a semi-analytical impactor geometry independent model to evaluate impaction velocity in a single-stage low-pressure impactor.

As the inertial impaction of nanosize agglomerates has been studied, the process has been inspected from the view of either the fragmentation or the bounce. However, to understand the overall

picture, both aspects, the fragmentation and the bounce, should be considered and examined simultaneously.

The focus of this thesis was to examine the break-up and bounce of agglomerates during inertial impaction experimentally. The key objectives were:

1) To design and build a measurement set-up that allowed the characterization of both deposited and bounced particles (**Paper I**)
2) Evaluate impaction velocities of agglomerates during impaction (**Paper II**)
3) To generate agglomerates with varying properties and perform impaction behavior measurements with these agglomerates (**Paper II, III and IV**)
4) To determine the effect of impaction surface materials on break-up and bounce processes (**Paper III**)

2 THEORY

The outcome of the inertial impaction of an agglomerate is determined by the interaction between the agglomerate and the surface and the interactions within the agglomerate, namely between the primary particles. More specifically, does the agglomerate break up to smaller fragments and/or does it or parts of it bounce (Fig 1). As the agglomerate collides onto a surface, the agglomerate and the surface may deform plastically or elastically. This elastic deformation is a temporary change of shape, which, after impaction, reverses back to its original shape, whereas the changes are irreversible in plastic deformation. The energy that is stored in elastic deformation plays a significant role in the bounce process of the particle. If the elastic limit, which is the yield strength, of the material is reached during impaction, then the material experiences plastic deformation, which is irreversible. Here, plastic deformations of the agglomerate occur at contacts between primary particles because those contacts are considered the weakest links in the agglomerate. Thus, the contact mechanics that describe the interactions within the agglomerate and between the agglomerate and the surface are important for the understanding of the impaction processes.

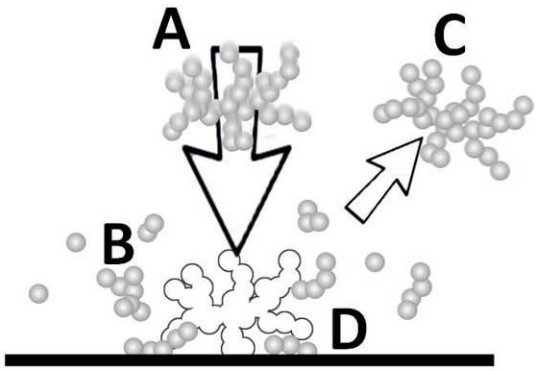

***Figure 1**. Schematics of the impaction process: A: Intact particles, B: fragmented and bounced particles, C: bounced and non-fragmented particles and D: deposited particles (non-fragmented or fragmented)*

2.1 Contact types

The contacts of agglomerated/aggregated nanoparticles may be based on electric or magnetic fields, or on material bridges between the contact surfaces (Fig 2). In addition to the Van der Waals contacts, the electric field produces the attractive contact force between the charged particles. Magnetic particles may produce magnetic contacts.

A material bridge between the contact surfaces may form in several ways. The solid bridges may be formed physically, e.g., through sintering, or through chemical reactions. A liquid may also form a bridge between the surfaces, which enforces the contact.

The Van der Waals forces between the particles are considered the weakest, and the solid bridges are considered the strongest. For further information, see, e.g., Reynolds et al. (2005).

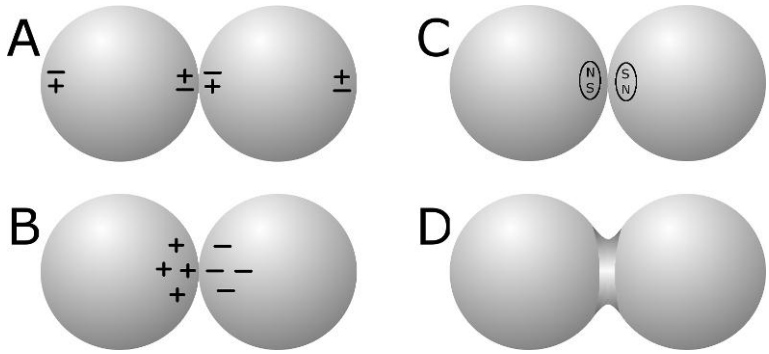

Figure 2. *Examples of different contact types between two particles. Bonding based on* ***A)*** *Van der Waals interactions,* ***B)*** *electrostatic forces,* ***C)*** *magnetic forces and* ***D)*** *liquid or solid bridge between the particles*

2.2 JKR (Johnson, Kendall and Roberts) theory for contacts

Adhesion causes an attractive contact force between the particle and the surface. To be able to estimate the strength of this contact, one must define the contact type between the particle and surface.

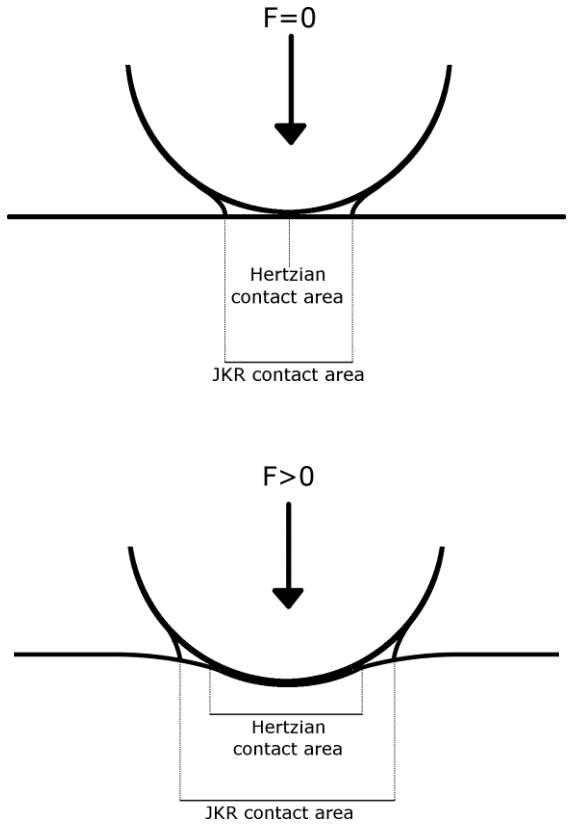

Figure 3. *Contact area, which is based on Hertzian and JKR theories, between a spherical object and a flat surface with and without external force*

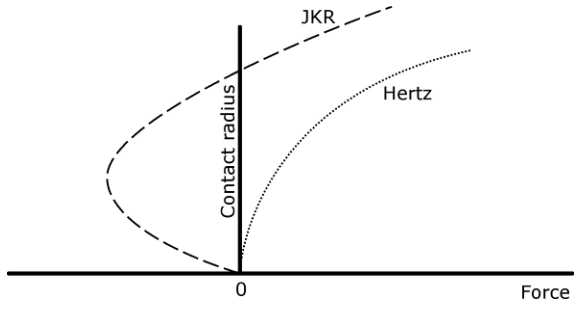

Figure 4. *Contact radius, which is based on Hertzian and JKR theories, between a spherical object and a flat surface as a function of external force. Positive external force is directed towards the surface (see Fig. 3)*

There are several theories attempting to explain the contact mechanics between two objects. One of the earliest theories is the Hertzian contact (Hertz, 1896), which describes the relation between the contact area and the elastic deformation of the bodies. However, the Hertzian model does not take into account contact adhesive interactions. To defeat this limitation, Johnson et al. 1971 described the JKR (Johnson et al., 1971) theory. This theory is based on the Herzian theory, with the addition of the adhesive contact interaction (Fig. 3 and 4). In the JKR theory, the contact area between two bodies is larger than zero when the bodies are in contact and when no external loads are applied. If an attempt is made to separate the objects, then an attractive force between the objects must be overcome. According to the JKR theory, the adhesion energy between two bodies can be defined as follows (Wang and Kasper, 1991):

$$E_{ad} = \frac{\sigma \pi d^2}{4}, \qquad [1]$$

where σ is the specific adhesion energy at the interfacial contact area, and d is the diameter of the contact area. The diameter of the contact area is defined as follows:

$$d = \left[9\pi^2 D_p{}^2 \sigma (K_S + K_P)\right]^{\frac{1}{3}}, \qquad [2]$$

where D_p is the diameter of the sphere, in the case of a sphere-surface interaction, and D_p=0.5*D_1D_2/(D_1+D_2), if two spheres with diameters D_1 and D_2, respectively, are in contact.

Other contact mechanic models are, e.g., the DMT theory (Derjaguin et al., 1975) and Bradley's model (Bradley, 1932). These models take into account the Van der Waals attractive force outside the elastic contact region, which is neglected in the models of JKR. The contacts were based on the JKR theory in this study because the

JKR theory has been widely used and tested and because the theory includes the adhesion between two objects.

2.3 JKR and agglomerate – surface interface

During an inertial impaction, a particle may stick onto the surface or bounce back to the gas flow. Whether the particle bounces depends on the adhesion relation between the particle and the surface, with the energy stored in the elastic deformations during the impaction process.

According to the JKR theory, the adhesion between two objects depends on their material properties, such as elastic modulus and specific adhesion energy. In addition to these properties, plastic deformation may change the shape of the particle, which will affect the contact area between these two objects. This change has a direct effect on the adhesion energy.

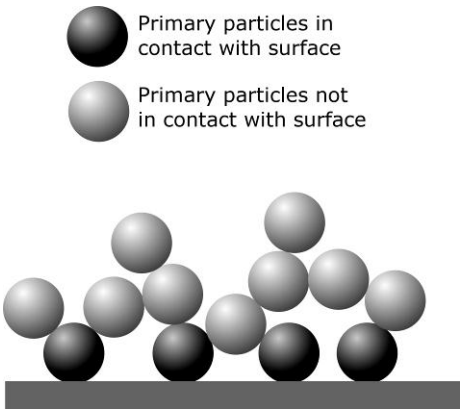

Figure 5. *Example of an agglomerate contacting a surface*

The adhesion between a sphere and a surface, according to the JKR theory, may also be applied to agglomerates, with a couple of assumptions. The contact between the agglomerate and the surface

occurs via primary particles. If M primary particles of the agglomerate are assumed to contact the surface (Fig. 5), then the total adhesion energy can be described as a sum of adhesion energies between these primary particles and the surface. If all the contacts are assumed identical, then the adhesion energy between the agglomerate and the surface may be described as follows:

$$E_{ad} = \frac{M\sigma\pi d^2}{4}, \quad [3]$$

$$d = \left[9\pi^2 {D_{pp}}^2 \sigma (K_S + K_P)\right]^{\frac{1}{3}} \quad [4]$$

2.4 The Weber number of an agglomerate

During impaction, energy is primarily consumed by elastic and plastic deformations. The elastic deformation and the rebound energy that is stored are the driving processes behind the bounce. In contrast, the adhesion, which may be affected by both plastic and elastic deformations between the particle and the surface, is the energy barrier that is required to overcome by the rebound energy. The energies during the impaction may be balanced as follows:

$$E_{kin,i} = E_{ad} + E_{kin,f} + L \quad [5]$$

where $E_{kin,\,i}$ is the initial kinetic energy, $E_{kin,\,f}$ is the final kinetic energy, E_{ad} is the adhesion energy difference between the inbound and bounce phases, and L includes the losses (Wang and Kasper, 1991; Wang and Flagan, 1990). The bounce tendency may be expressed with a Weber number We which describes the ratio of the kinetic energy available for the bounce to the adhesion energy needed to overcome for the particle to bounce. Because the relation of the losses L and the initial kinetic energy may be described with the coefficient

of restitution, $e^2=1-L/E_{kin,i}$ the Weber number may be written as follows:

$$We = \frac{E_{kin,i}e^2}{E_{ad}} \qquad [6]$$

By combining the equations [3], [4] and [6], and by assuming that the mass of the agglomerate is the sum of the masses of N primary particles, the Weber number for an agglomerate impacting at velocity v can be written as follows (**Paper III**):

$$We_{aggl} = \left(\frac{M}{N}\right)^{-1} \frac{e^2 D_{pp}^{\frac{5}{3}} \rho_{bulk} v^2}{9^{\frac{7}{6}} \sigma^{\frac{5}{3}} \pi^{\frac{4}{3}} (K_S + K_P)^{\frac{2}{3}}}. \qquad [7]$$

The ratio of M to N describes the number fraction of the primary particle in contact with the surface and it decreases as the agglomerate size increases (this is shown in **Paper III**).

Plastic deformations, e.g., the break-up of the agglomerate, affect the bounce. Three simplified scenarios may occur in which strong plastic deformations and the bounce can be observed (Fig. 6).

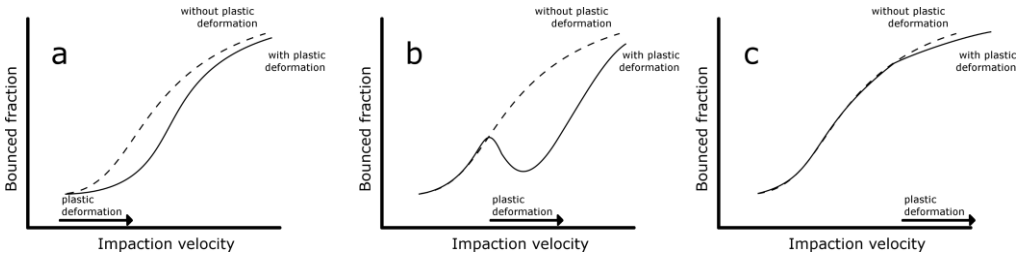

***Figure 6**. Bounce probability in three different cases in which plastic deformation occurs (**Paper III**). a) the particles plastically deform at the same or lower velocities than bounce would begin to occur. b) the particles*

first start to bounce; however, as the impaction velocity further increases, plastic deformation occurs. c) plastic deformation occurs at high enough impaction energies

1) The particles strongly deform at the same or lower velocities than bounce would begin to occur. Here, the plastic deformation that is experienced by the particles decreases the tendency to bounce and, thus, increases the critical velocity for the bounce.
2) The particles first start to bounce; however, as the impaction velocity further increases, strong plastic deformation occurs. As the particles plastically deform, adhesion increases, and energy is consumed on the deformation itself. Thus, it is possible that the bounce rate decreases until the increasing impaction energy overcomes the energy loss on the plastic deformation. Awasthi et al. (2007) found this bimodal trend while simulating the rebound and adhesion behavior of Lennard-Jones clusters.
3) Plastic deformation occurs at high enough impaction energies where there is excess energy available for the bounce. Here, fragmentation would not have a significant effect on the bounce.

As a particle impacts onto a surface, the two materials interact with each other. Thus, in addition to particle properties, the properties of the impaction surface may affect the outcome of the impact. The surface material properties may affect the outcome in several different ways. First, the adhesion between the particle and surface affects the elastic energy that is required for the bounce. Then, the elasticity of the surface material affects the force that the particle will experience. Finally, charge transfer may occur during the impaction and bounce. These possibilities are considered in **Paper III**.

3 METHODS

3.1 Experimental

The experimental set-up (Fig. 7) was designed and built to fulfill the following requirements. First, the characterization of both deposited and bounced particles should be possible using this system. Second, the analysis of bounced particles using online measurement devices is also desirable. The method would then decrease the time consumption of the analysis compared with the more traditional TEM analysis.

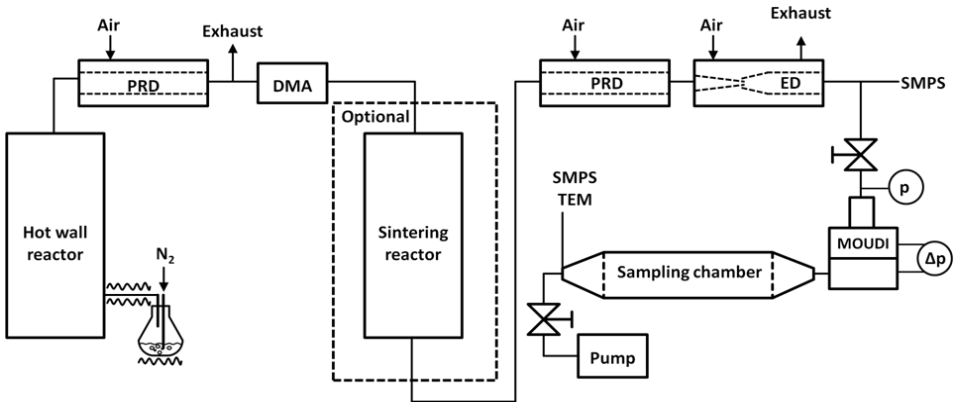

Figure 7. *The measurement set-up*

A combination of a differential mobility analyzer (DMA; TSI inc.), a single-stage micro-orifice uniform deposit impactor (MOUDI) and a low-pressure sampling chamber were used to study the break-up and bounce of the agglomerates. In this method, the generated

agglomerates were first size-classified using a DMA to produce a monodispersed size distribution, which was then introduced to the MOUDI for the impaction process. The pressure conditions after the MOUDI were below the atmospheric pressure. Thus, to be able to analyze the bounced particles after the impactor, with the measurement devices working at atmospheric pressure, the low-pressure sample had to be converted back to the atmospheric pressure. For this purpose, a novel sampling chamber was designed and used. This chamber allowed the semi-online measurement of the bounced particles from low pressure.

In addition, samples for TEM were collected using an aspiration sampler (Lyyränen et al., 2009) on copper-supported carbon films with holes. The deposited particles were also collected for a later analysis on a TEM-grid, which was on the impaction plate. To characterize the intact particles, the same analysis and sampling procedure were performed without the impaction plate.

Figure 8. *Single-stage MOUDI*

3.1.1 Micro-orifice uniform deposit impactor

A single-stage MOUDI (MSP corp.; Marple et al., 1991) was used as an impaction platform (Fig. 8). The stage contained 2000 orifices with an approximate diameter of 55 μm. The impaction plate was covered with aluminum foil, which was used as a default impaction plate material. A small hole (smaller than the TEM-grid) was cut to the aluminum foil, and a TEM-grid was placed between the foil and the plate at the position of the hole. This set-up enabled a sample collection for the TEM-analysis. The aluminum foil was also covered with other metals using the sputtering technique to determine the effect of impaction surface material on the impaction outcome. During the impaction, the impaction surface may already contain a particle that was deposited earlier at the location of the current impact. To reduce the probability of this scenario, the impaction plate was rotated at constant time intervals, which, thus, allowed an even deposition of the particles on the entire impaction surface. The estimated coverage of the area by particles was 3-10 % during this study.

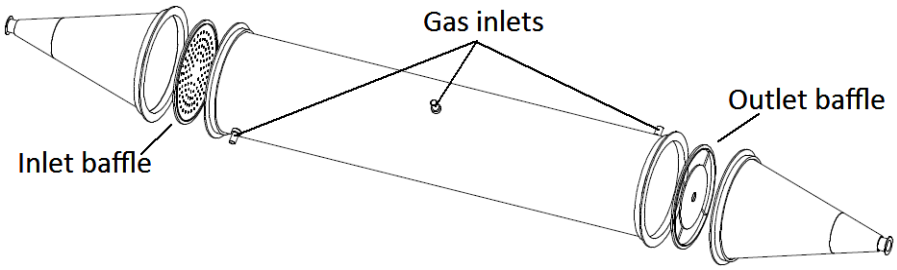

Figure 9. *Scheme of the low pressure sampling chamber*

3.1.2 Low-pressure sampling chamber

A low-pressure sampling chamber (Fig. 9) was designed and built to enable the sampling of the bounced particles. During the sampling phase, the low-pressure sample was carried through the sampling chamber until the chamber, which had a volume of approximately 60 l, was saturated with the aerosol sample. The saturation process was aided by increasing the mixing in the chamber using baffles.

The basic principle of the operation of the sampling chamber was as follows:

1. The low-pressure aerosol sample flow from the impactor was introduced into the sampling chamber.
2. The outlet of the chamber was closed with valves.
3. The chamber was pressurized to ambient conditions with filtered air.
4. A sample was taken for the aerosol analyzers and for the TEM grid. The chamber pressure was maintained with filtered air, which was introduced to the chamber at both ends.

The sampling chamber design was optimized by Computational Fluid Dynamics (CFD) modeling to solve the flow field in the sampling chamber during the sampling phase, i.e., in the conditions where the sample is introduced from the impactor into the chamber (**Paper I**). In addition, experiments were performed to test the performance of the chamber and to answer the following questions: What is the gas volume that needs to be sampled to saturate the chamber to a uniform aerosol concentration? Is the number size distribution constant after the pressurizing process, in which the sample is pressurized to the atmospheric pressure? When taking the sample from the chamber, how do the number size distribution and particle concentration change over time due to particle losses? These questions have been considered in **Paper I**.

3.1.3 Chemical vapor synthesis

Chemical vapor synthesis (CVS) (Kodas, 1999; Lähde et al., 2011; Miettinen et al., 2009) was applied for the generation of TiO_2, copper and iron oxide agglomerates in this thesis. A common generation setup for CVS is presented in Fig. 7. The precursor was vaporized at the desired temperature, which was controlled with the help of a heated water bath. The vaporized precursor was then carried with a carrier gas, which was typically nitrogen, to a laminar hot wall reactor. The hot wall reactor consisted of a tube, heat elements and a control unit. The feeding line before the reactor was also heated and insulated to avoid condensation of the precursor material to the walls of the line. In the reactor, the precursor material was thermally decomposed, and primary particles were formed by nucleation. Due to nucleation, coagulation, and agglomeration, the agglomerates were generated. The aerosol generation process was quenched by applying a dilution air with a porous tube diluter, as described previously by Lyyränen et al. (2004).

In the case where a higher degree of sintering between the primary particles of TiO_2 agglomerates was desired (see, e.g., Eggersdorfer et al., 2011), an additional hot wall reactor was used in the measurement set-up after the size classification of the particles (Fig. 7). The residence time in the sintering reactor was controlled using the volume flow rate through the reactor.

Iron oxides with two different oxidation states were used: hematite and magnetite. The oxidation state was controlled by regulating the amount of oxygen in the reactor. The oxygen controlled iron oxide generation has been investigated in the **Paper IV**.

3.2 Impaction velocity simulations

The impaction velocity is one of the key parameters because this parameter defines the available energy for the processes that occur during impaction. The impaction velocities of the agglomerates were estimated using a combined method of computational fluid dynamics (CFD) simulations and Lagrangian particle trajectories. This method is based on the work by Arffman et al. (2011), who estimated the D_{50} cutoff sizes of an electrical low pressure impactor (ELPI plus).

The flow of a single nozzle of the MOUDI was modeled in two dimensions using the SST-k-ω-turbulence transfer model (Menter, 1994) and the advanced wall treatment of the ANSYS Fluent 12.1.4 software (ANSYS inc.). The particle trajectories were calculated by integrating their equation of motion using an Eulerian method and the flow field data obtained by CFD. The equations of motion were:

$$\vec{v}(x_1, y_1) = \vec{v}(x_0, y_0) + \vec{a}(x_0, y_0)dt$$
$$(x_1, y_1) = \vec{v}(x_0, y_0)dt + (x_0, y_0) \quad [8]$$

where v and a indicate the two-dimensional particle velocity and acceleration, respectively, at a given location (x_0,y_0) and after the time step dt at location (x_1,y_1).

The acceleration of the particle was estimated with the drag force F_d, which can be expressed for spherical particles as follows:

$$\overrightarrow{F_{d,s}} = \frac{3\pi\eta\Delta\vec{v}d}{C_c(d)}, \quad [9]$$

where n is the viscosity of the gas and Δv is the differential velocity between the particle of diameter d and the medium gas. C_c represents the Cunningham slip correction factor for the particle. An impactor

classifies particles according to their aerodynamic size, i.e., the diameter of a spherical particle with unit density that has the same terminal velocity under gravity as the original particle. Therefore, the acceleration of the particle in the flow field was modeled as follows:

$$\vec{a} = \frac{18\eta\Delta\vec{v}}{d_a^2 C_c(d_a)\rho_0}. \qquad [10]$$

The outcome of the particle tracking simulations is that one can obtain the impaction velocities of particles as a function of their aerodynamic size. However, as real particles may have an irregular shape, it was necessary to convert the electrical mobility sizes to aerodynamic sizes. This conversion can be performed with the following relation (Kelly and McMurry, 1992):

$$d_a = d_b \sqrt{\frac{C_c(d_b)}{C_c(d_a)} \frac{\rho_{eff}}{\rho_0}} \qquad [11]$$

where ρ_{eff} is the effective density of the particles, and ρ_0 is the unit density. The effective density can be measured using a combination of the aerosol particle mass analyzer (APM) and the DMA, as described by Park et al. (2003), and the electrical mobility can be measured using the scanning mobility particle sizer (SMPS).

3.3 Agglomerate characterization

The intact agglomerates were characterized using online methods for their size (electrical mobility, SMPS) and mass (APM). This characterization enabled the estimation of the fractal dimensions and the size dependent effective densities of the agglomerates. This

estimation was crucial because the effective density and its dependence on size (fractal dimension) were used to characterize the agglomerate during impact velocity simulations and to convert number size distributions to mass concentrations. Further, the SMPS was used to obtain the size distribution of the bounced fragments of the agglomerates after the impaction. In addition to the online methods, the surface area equivalent diameters of the intact and bounced agglomerates were analyzed using TEM.

3.3.1 Scanning mobility particle sizer

The electrical mobility number size distribution was analyzed using a Scanning Mobility Particle Sizer (TSI inc.), which is a combination of a neutralizer, differential mobility analyzer (DMA) and a condensation particle counter (CPC) (Wang and Flagan, 1990). The operation principle of the SMPS is as follows: before entering the DMA, the particles are charged with a natural charge distribution by the neutralizer. In the DMA, the particles are carried by the airflow between two coaxial cylinders with a voltage potential difference. The particles experience a Coulomb force, which drive them toward the inner wall of the DMA due to the electric field. As the air resists this movement as a drag force, the forces balance each other out, and the particle travels toward the wall at a constant velocity according to the electrical mobility of the particle. The particles of certain electrical mobility are able to travel to the sample exit point, from which the monodispersed population is carried to the CPC for number concentration measurements. By changing the voltage of the DMA, the desired size range of the particles and their corresponding concentrations, i.e., the electrical mobility number size distribution, can be scanned.

3.3.2 Aerosol particle mass analyzer

The aerosol particle mass analyzer (APM) classifies the particles by their mass to charge ratio (Ehara et al., 1996). The APM consists of two rotating coaxial cylinders with a cap and an electric field between the cylinders. As a charged particle moves through the APM, the centrifugal force drives the particle toward the outer cylinder, and the electric field induces a Coulombic force toward the inner cylinder. If these forces balance out, then the particle is not driven to the walls and, thus, is able to exit the APM. The APM classifies the particles by their electric charge to the mass ratio. For singly charged particles, the APM classifies the particles by their mass.

3.3.3 Measurement method for effective density

The ability to classify the particles by mass (APM) and electrical mobility (SMPS) was exploited to evaluate the size-dependent effective densities of the agglomerates. The particles were first run through the APM, and the size distribution of the mass-classified particles was then measured with the SMPS. By applying a lognormal fit for the SMPS data, the mode value for the electrical mobility was found. By changing the APM voltage setting, the electrical mobility diameter of agglomerates of different mass could be obtained. A similar system has been previously used by, e.g., Malloy et al. (2009); McMurry et al. (2002).

3.3.4 Transmission electron microscopy

The intact particles and the bounced particles were collected for TEM (JEM-2100F, JEOL Ltd.) analysis using an aspiration sampler (Lyyränen et al., 2009), which was on holey carbon copper grids (Agar Scientific Inc. S147-400 Cu). The deposited particles were also collected for TEM analysis on carbon film on copper mesh grids

(S160-400 Cu), which were located on the impaction plate during the measurements.

3.3.5 Fractal dimension and effective density

The fractal dimension $D_{f,gyr}$ describes the power law relation between the radius of gyration d_{gyr} and the number of primary particles N (Mandelbrot, 1983):

$$N = C\left(\frac{d_{gyr}}{d_{pp}}\right)^{D_{f,gyr}} \qquad [12]$$

where d_{pp} and C are the radius of the primary particle and a prefactor, respectively. This fractal dimension is based on the radius of gyration. An analogous power law has been used to describe the relation between the mass m and the electrical mobility diameter d_e of the agglomerate (Park et al., 2003):

$$m = C\left(\frac{d_e}{d_{pp}}\right)^{D_f} \qquad [13]$$

As the effective density ρ_{eff} can be defined using the mass and the electrical mobility as follows (Park et al., 2003):

$$\rho_{eff} = \frac{m}{(1/6)\pi d_e^{\,3}} \qquad [14]$$

The relation between the effective density, electrical mobility diameter and the mass-based fractal dimension can be written as follows (Park et al., 2003):

$$\rho_{eff} = D' d_e^{D_f - 3} \qquad [15]$$

3.3.6 Mass-based bounce fraction

The mass concentration of the intact and bounced particles was calculated using the number size distributions and with the size-dependent effective density. The noise of large particle data in the SMPS, however, produces oscillating results due to the power of three (with spheres) relation between diameter and the mass. To cancel out this error, the number size distribution data of the SMPS were fitted to lognormal distributions using the least squares method. There were two modes in the fitting of intact particles, which described the singly and doubly charged particles. The size distribution of the bounced particles was fitted to three modes. One mode described the broken fragments, and the other two modes described the singly and doubly charged intact particles, which did not fragment during impaction.

4 RESULTS AND DISCUSSION

4.1 Impaction velocity results

To estimate the impaction velocities, the trajectories of the particles in a MOUDI were simulated (**Paper II**). The impaction velocity was affected by the operation conditions of the MOUDI (pressure difference over the jet plate) and by the particle aerodynamic diameter. In Fig. 10, the simulated maximum velocity of the particle in the jet and the impaction velocity of the particle are presented for the case in which the pressure difference in the impactor was 250 mbar, i.e., the highest value that was applied during the measurements. The figure shows that, as the aerodynamic diameter increases, the impaction velocity also first increases. This increase is due to the higher inertia and thus stronger impaction of the particle as the aerodynamic diameter becomes larger. At the same time, however, the acceleration of the particle in the jet before the impaction plate also decreases due to the inertia as the aerodynamic diameter is increased resulting in lower maximum velocity. These two competing phenomena cause the maximum in the impaction velocity curve as shown in Fig. 10.

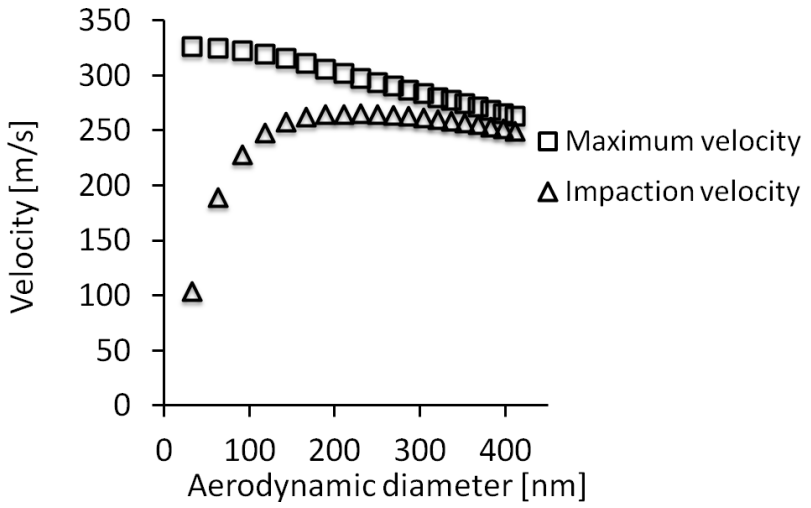

Figure 10. *Simulated maximum particle velocity and impaction velocity as a function of aerodynamic diameter. The pressure difference was 250 mbar*

The impaction velocities of the particles, which were normalized using the average jet gas velocity at different pressure differences over the impactor, are shown in Fig. 11. Marple (1970) used simulations to demonstrate that, at high Stokes region, the ratio of the impaction velocity to the average jet velocity is 0.85. This relation has been used to estimate the impaction velocities in studies of the impaction behavior of nanoparticles. However, as the simulation results in Fig. 11 show, this relation overestimates the impaction velocity at lower Stokes values. As the Stokes number increases, the ratio reaches the maximum value of 0.9.

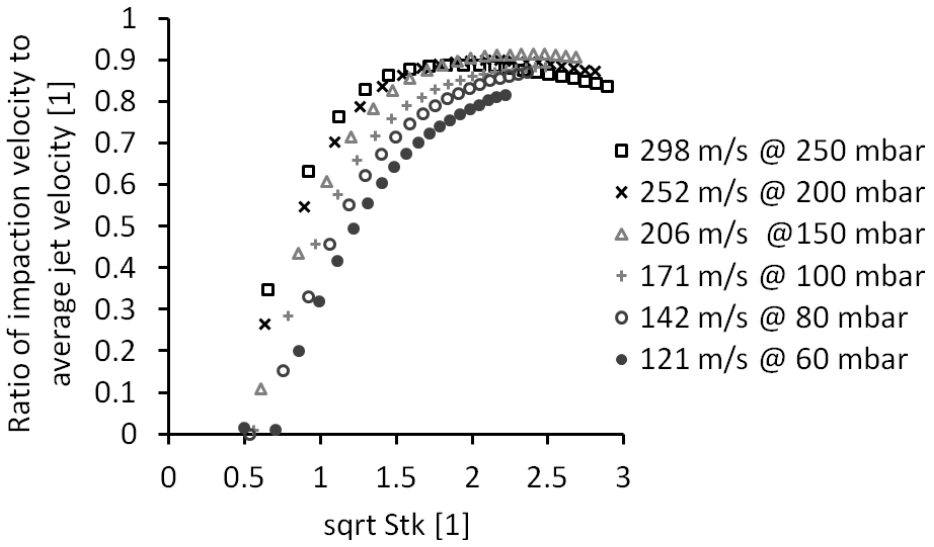

Figure 11. *Ratio of the impaction velocity to the average jet velocity. The average jet velocity at the given pressure difference is shown in the legend. The square root value of Stokes number (x-axis) is proportional to the particle diameter*

4.2 Agglomerate and system properties that affect the fragmentation and bounce

The fragmentation and bounce of nano agglomerates of different properties were studied in **Papers II** and **III**. The effects of the degree of sintering, primary particle size, agglomerate size and agglomerate material were experimentally explored. The results are shown in Figs 12-17 and in Tables 1 and 2. In the following section, we interpret the results and discuss the implications of the results.

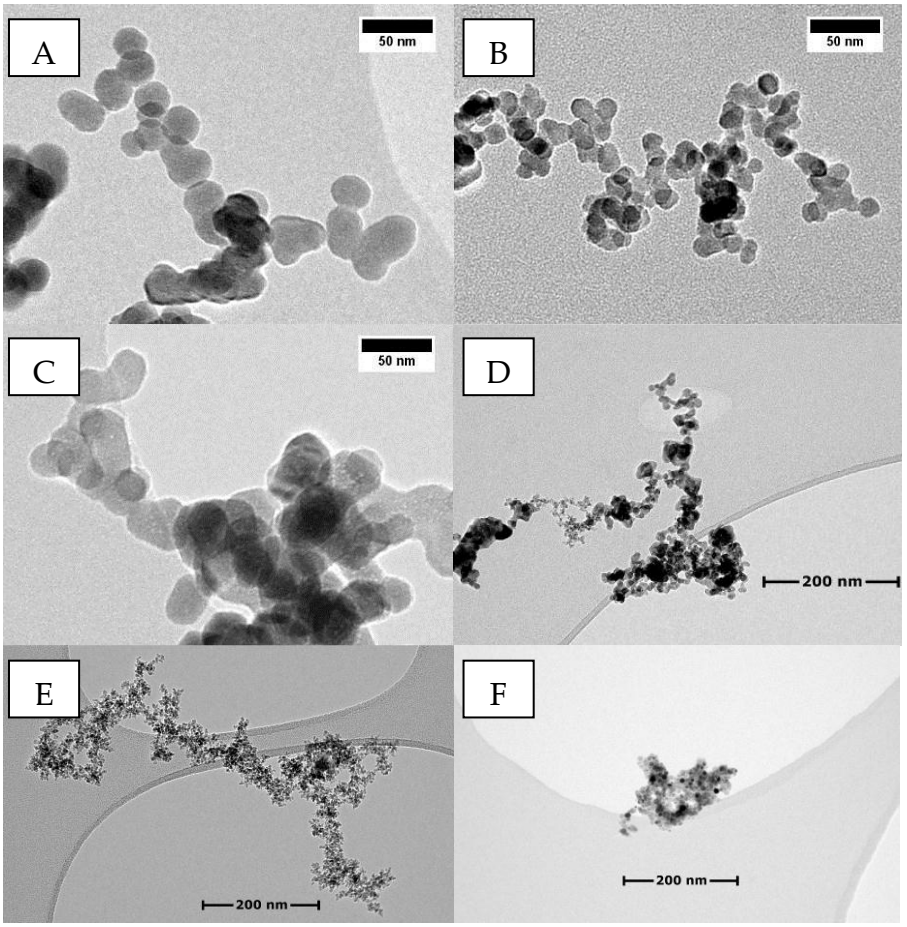

Figure 12. *TEM micrographs of* ***A)*** *TiO_2 (base case),* ***B)*** *TiO_2 (smaller primary particle size),* ***C)*** *TiO_2 (higher degree of sintering),* ***D)*** *magnetite,* ***E)*** *hematite and* ***F)*** *copper agglomerates*

4.2.1 The agglomerates

The impaction behavior of agglomerates with different properties was studied experimentally. The agglomerate material, agglomerate size, primary particle size and the degree of agglomerate sintering were varied to explore their effect on fragmentation and bounce

during the inertial impaction. The agglomerate types are shown in Table 1, and the TEM micrographs are shown in Fig. 12.

Table 1. *Agglomerate properties that were used in this study*

Material	***Agglomerate size [nm]***	***Primary particle size [nm]***
TiO_2	*250, 300, 400*	*27*
TiO_2	*250*	*16*
TiO_2	*250*	*27 + sintering*
Magnetite	*250*	*10*
Hematite	*250*	*5*
Copper	*150*	*<10*

4.2.2 Impaction velocity

The size distributions of the bounced TiO_2 particles as a function of impaction velocity are presented in Fig 13. Increasing the impaction velocity decreased the average size of the bounced particles and increased the number concentration. Three distinct features were observed in the results. First, the geometric mean diameter (GMD) (Fig. 13) of the bounced particles depended on the particle type and on the impaction energy. Up to 27 bonds broke up at the highest impaction velocity (Fig. 15), which indicated that the agglomerates fragmented into up to 28 pieces. Second, the change in the bounced particle size decreased as the impaction energy increased. Third, all of the agglomerates did not break up for the cases of smaller primary particle size and a high degree of sintering (Fig. 14). Similar results were obtained also for iron oxide agglomerates.

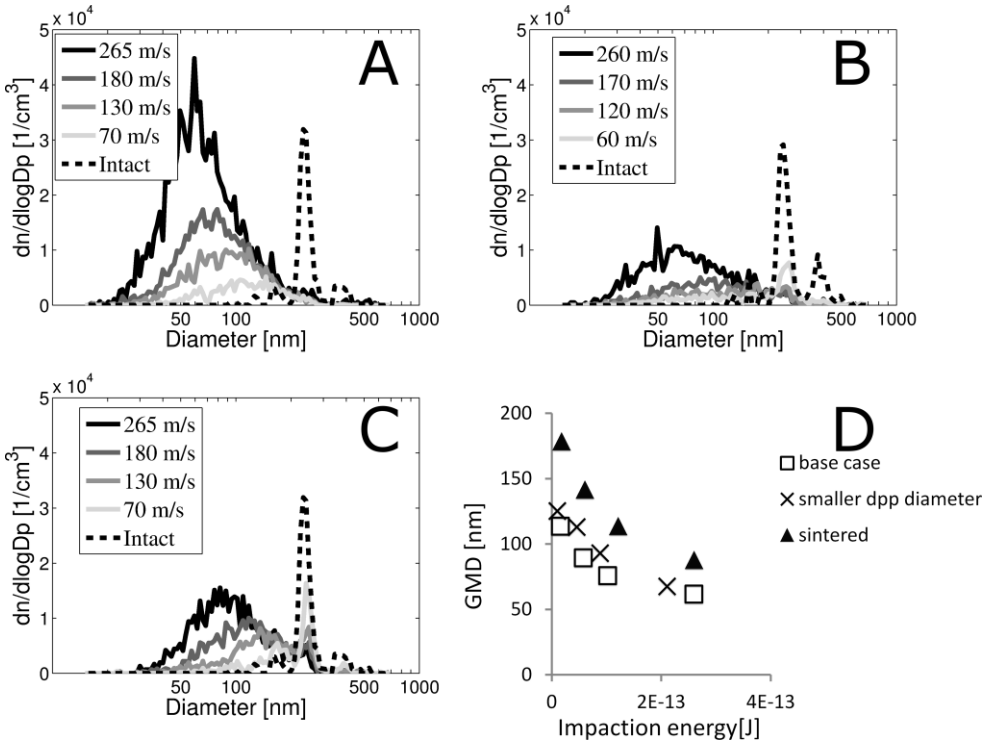

Figure 13. *Measured size distributions of the bounced TiO_2 fragments. A) TiO_2 (base case), B) TiO_2 (smaller primary particle size), C) TiO_2 (higher degree of sintering) and D) geometric mean diameter of bounced and de-agglomerated particles measured with SMPS*

4.2.3 Degree of sintering (Paper II)

The effect of the degree of sintering was evaluated by increasing the degree of sintering of generated TiO_2 agglomerates and by comparing the impaction results to the base case. The results in Figs. 13-14 show that increasing the degree of sintering affected both the fragment size and the mass-based bounce fraction. The sintering that was applied to the agglomerates strengthened the bonds between the primary particles, which resulted in less broken bonds per agglomerate due to

the impaction (Fig 15). In addition, a significant fraction of the agglomerates that bounced were non-fragmented.

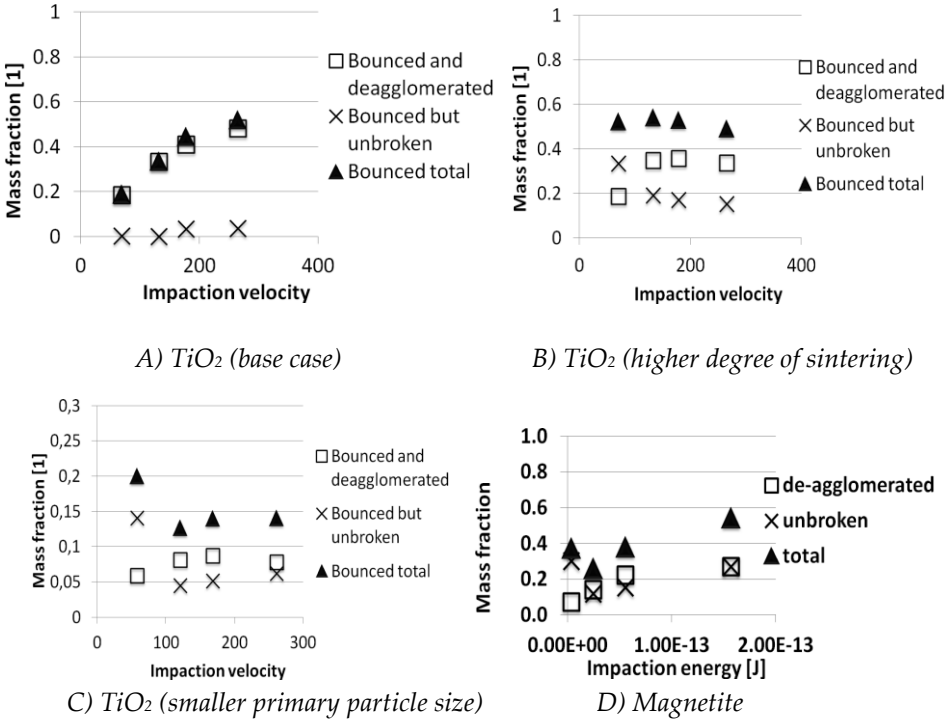

Figure 14. *Mass fractions of the bounced TiO_2 and magnetite agglomerates*

The mass-based bounce fraction remained at an approximately constant level through the impaction energy range. Two modes were visible: non-fragmented and fragmented particles. The non-fragmented particles dominated the bounced fraction at the lowest impaction energy, and the broken fragments became dominant as the energy was increased.

4.2.4 Primary particle size (Paper II)

Decreasing the primary particle size of TiO_2 agglomerates from 27 nm to 17 nm slightly increased the fragment size of the bounced particles at the same kinetic energy (Fig. 13), and thus, approximately the same number of bonds broke during the impaction (Fig. 15). However, the degree of fragmentation decreased significantly. This decrease was due to the higher number of intact bonds in an agglomerate of smaller primary particle size than in the case of larger primary particles.

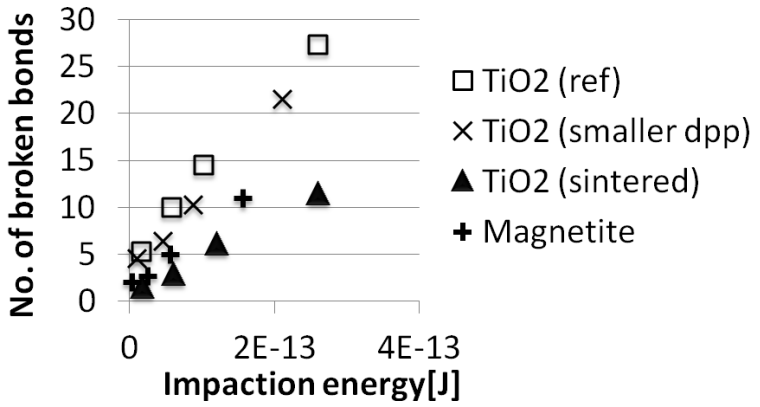

Figure 15. *Number of broken bonds per agglomerate*

The bounce fraction decreased significantly when the primary particle size was smaller (Fig. 14). This significant decrease may be attributed to smaller primary particle size; however, the exact process remains unknown. The ability to store elastic energy by an agglomerate with a smaller primary particle size compared with an agglomerate with larger primary particle size may be one potential reason.

4.2.5 Agglomerate size (Paper II)

The results of the impaction study of TiO_2 agglomerates of different electrical mobility size are shown in Table 2, in which the same pressure difference over the jet plate was maintained at a constant. There were no significant changes in the fragment size or kinetic energy per broken bond, although the intact particle size varied from 250 nm to 400 nm. Two main factors affected this result. The first factor is the increased number of bonds in larger intact agglomerates; more bonds must be broken to achieve a certain fragment size than in the case of smaller intact agglomerates. The number of bonds in an agglomerate can be estimated as directly proportional to the mass of the agglomerate. In contrast, the available kinetic energy is directly proportional to the mass of the agglomerate. Thus, the additional mass provides the extra energy that is required for the larger intact agglomerate to fragment to the same size of fragments as the smaller intact agglomerate fragments.

Table 2. *Geometric mean diameters of the bounced particles that were measured using the SMPS for a 150 mbar pressure difference*

Case	***Base case, 250-nm agglomerate***	***300-nm agglomerate***	***400-nm agglomerate***
Intact agglomerate size [nm]	*250*	*300*	*400*
GMD [nm]	*78*	*80*	*79*
E/broken bond [1e-14 J]	*1.1*	*1.0*	*1.2*

4.2.6 Agglomerate chemical composition (Paper III)

In addition to the TiO_2 agglomerates, the impaction behavior of the iron oxide particles was also experimentally determined. The oxidation state of iron was controlled during the production phase, and impaction experiments were conducted for both iron oxide types: magnetite and hematite. However, because the results were

extremely similar in both cases, only the results for magnetite are shown here. With magnetite particles, the bounce fraction reached its minimum at the second lowest impaction energy (Fig. 14). As the energy was increased beyond this level, the bounce fraction increased.

As in the cases of smaller primary particle diameter and a higher degree of sintering for TiO_2, both the non-fragmented and fragmented magnetite particles were observed, and the overall bounce fraction behavior depended on these two modes and on how these two modes compare with each other. With magnetite particles, these modes were quite separate, which resulted in a notch to the total bounce fraction. In that notch, the adhesion and energy consumption due to the plastic deformations overcame the increased impaction energy, which resulted in a lower bounce fraction than at the lower impaction velocity. This was affected by the increased relative adhesion due to fragmentation of the agglomerate and the energy consumption during fragmentation. Similar behavior was also found for TiO_2 with smaller primary particle size.

The copper particles were impacted only at the highest velocity that was available; however, still there was no significant particle bounce. The average projected area equivalent diameter values, which were analyzed using TEM micrographs of the deposited particles (Fig. 16) show that only small fragments disintegrate from the intact agglomerates. This produces a bimodal distribution of large and small deposited particles.

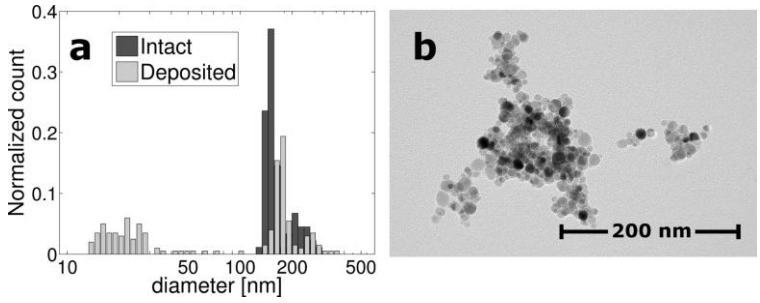

Figure 16. A) *Projected area equivalent size distributions of deposited and intact copper agglomerates.* ***B)*** *TEM image of the deposited copper agglomerate*

4.2.7 Impaction surface material (Paper III)

TiO_2 and magnetite agglomerates were impacted on the impaction surfaces of aluminum, titanium, silver, copper and iron. Fig. 17 shows the fragment size of the bounced particles and the mass-based bounce fractions. Although the impaction surface materials had quite different properties with respect to surface adhesion, elasticity and tendency for the charge transfer, the results suggest that the impaction plate materials that were used during this study did not have a significant effect on the break-up or the bounce. It has been reported that the impaction plate material does affect the particle bounce when the impaction velocities are low Wall et al. (1990). However, when the impaction velocities are higher, the effect of the plate material diminishes. This observation is further confirmed here experimentally because the impaction velocities were quite high in this study. Salman et al. (2002) found in their impact fragmentation study of over a millimeter particles that, if the target material was thin enough, then the fragmentation decreased due to the bending of the target material. These researchers found this effect on the target material thickness of less than 5 mm, whereas the impacting particle's diameter was approximately 5 mm.

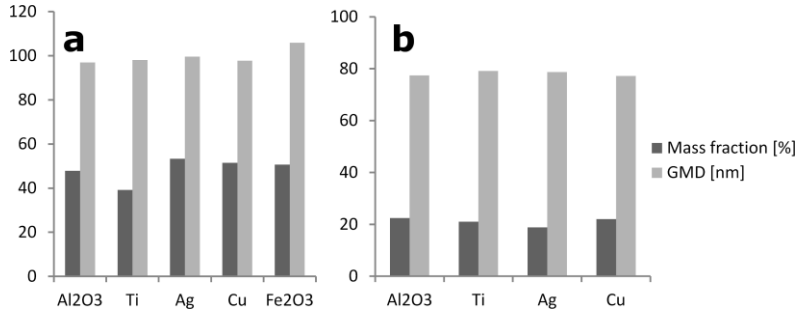

Figure 17. *The bounce fraction and the GMD values of the bounced and de-agglomerated* ***A)*** *magnetite and* ***B)*** *TiO_2 particles with impaction surface materials of Al2O3, Ti, Ag, Cu, Fe_2O_3*

5 REVIEW OF THE PAPERS

Paper I describes and tests a method for the simultaneous investigation of the fragmentation and bounce of the aerosols during impaction. The lack of knowledge regarding simultaneous bounce and fragmentation is the motivation for the development of the new novel method. The method was used to impact TiO_2 agglomerates at one impaction velocity, and deposited and bounced fragments were characterized.

In **paper II**, the method that was described in **Paper I** was applied to study the impaction behavior of TiO_2 agglomerates with different properties. The primary particle size, degree of sintering and agglomerate size were varied to determine how these changes affected the fragmentation and bounce during inertial impaction. A higher degree of sintering was found to increase the fragment size because the interparticle contacts were strengthened due to the sintering process. The agglomerates and their fragments were found to prefer to stick to the surface as the primary particle size was decreased. It was also evident that some of the agglomerates bounced, but did not fragment, during the impaction process. To be able to estimate the initial kinetic energy before impaction, the impaction velocities of the agglomerates were evaluated by simulating the particle trajectories in the impactor using the combined methods of CFD and Lagrangian path calculation.

Paper III concentrated on the bounce of the iron oxide agglomerates compared with those agglomerates of TiO_2. As the impaction energy increased, two competing mechanisms affected the outcome of the bounce: the increased adhesion and energy dissipation due to the plastic deformation and the increased energy that was available for the bounce. The result was that the bounce fraction was not always monotonically increasing. In **Paper III**, the

effect of the impaction surface material was also examined. This material was not found to have a significant effect on the break-up and bounce processes at the conditions that were used in **Paper III**.

In **Paper IV**, the generation of iron nanoparticles with controlled oxidation states in an aerosol phase was studied. The atmospheric pressure chemical vapor synthesis was applied, and magnetite and hematite were synthesized by controlling the amount of oxygen in the reactor. In addition to the empirical measurements, thermodynamic equilibrium calculations and CFD model were used to predict the oxidation state and the reaction conditions.

6 CONCLUSIONS

Understanding the processes during an inertial impaction of an agglomerate is crucial in aerosol technology fields that involve, e.g., aerosol transport or aerosol measurements. There are few studies regarding fragmentation during inertial impaction, particularly for nanosize particles, and studies regarding bounce of nanosize particles are even rarer. Nevertheless, during the inertial impaction, both aspects are important and co-exist. This thesis sheds light on the impaction behavior of nanosize agglomerates by considering both fragmentation and bounce.

A measurement system was designed and built to study the inertial impaction of nano particles and to characterize the deposited and bounced particles simultaneously. With this method, the inertial impaction of agglomerates of varying properties was inspected.

The agglomerate properties had an effect on their impaction behavior. For example, the bounced fraction decreased but the fragment size did not change notably as the primary particle size was decreased. Enhanced degree of sintering increased the fragment size due to stronger bonds between the primary particles. At the lowest impaction velocity, a considerable fraction of the agglomerates bounced without fragmentation at the lowest impaction velocity in most cases.

Some of the particles did not fragment during impaction. This phenomenon was observed, e.g., in the case where a higher degree of sintering between the primary particles was used to increase the strength of contacts. The fraction of the non-fragmented agglomerates was the highest at the lowest impaction velocities, where the available kinetic energy was the lowest.

An important observation was that the bounce fraction did not increase with the increasing impaction velocity in every case. This

was probably due to increased adhesion between the agglomerate and the surface that arises from the fragmentation. In addition, the fragmentation process reduces the energy available for the bounce. The agglomerate size was found to have little effect on the fragment size that resulted from the fragmentation. The intact agglomerates of 250 nm, 300 nm and 400 nm produced approximately the same average fragment size. This result was because the kinetic energy of the agglomerate increased as the size, and the mass, of the particle increased. Finally, approximately the same amount of energy (1 – 1.2 e-14 J) was estimated to be used per broken bond in each size fraction of an agglomerate.

The impaction plate material had little effect on either the fragmentation or the bounce. However, only metallic impaction surface materials were used and the velocities were relatively high.

Many of the basic phenomena that take place during the impaction of nanosize agglomerates were studied. However, not all the parameters that are involved in the impaction process, such as the impaction angle and surface roughness, were covered and, thus, require further work. The physics behind the processes are far from simple, and theoretical framework describing the processes and outcome of inertial impaction, which include both the deformation of the agglomerate and bounce, is not easily obtained. Thus, one of the key aspects that requires more work is the coupling of the experimental results to simulation models. This coupling would allow a better understanding of the processes that are involved and could ultimately give the tools for the predictions of the impaction behavior of agglomerates with arbitrary properties. These predictions would be useful for, e.g., determining how substantial the effect of the break-up and bounce of nuclear aerosols has on aerosol release in severe nuclear accidents.

In the future, one interesting application of the experimental device developed here is the online detection of the properties of various agglomerates. For example, in the engineered nanoparticle manufacturing processes, it is important to know whether the process

produces “hard” or “soft” agglomerates. Additionally, the methods that are described in this thesis can be utilized for online primary particle determination. Both of these applications may be important for e.g. combustion or aerosol-based nanomaterial synthesis purposes and makes the process control much faster than is currently possible with offline analysis methods.

AUTHOR'S CONTRIBUTION

In **Papers I**, **II**, and **III**, I performed the design of the measurement set-ups and performed the measurements. I also conducted the numerical simulations in **Papers I** and **II** and performed all the analyses, except for the TEM imaging, in the first three papers. I wrote most of the texts for these papers, except for the description of the impaction velocity simulation in **Paper II** and the description of TEM in **Papers I** and **II**. In **Paper IV,** I participated the planning and execution of the experiments and data interpretations.

REFERENCES

Abd-Elhady, M. S., Rindt, C. C. M., Wijers, J. G., van Steenhoven, A. A. (2006). Modelling the impaction of a micron particle with a powdery layer. *Powder Technol.* 168, 3:111-124.

Arffman, A., Marjamaki, M., Keskinen, J. (2011). Simulation of low pressure impactor collection efficiency curves. *J.Aerosol Sci*. 42, 5:329-340.

Awasthi, A., Hendy, S. C., Zoontjens, P., Brown, S. A., Natali, F. (2007). Molecular dynamics simulations of reflection and adhesion behavior in Lennard-Jones cluster deposition. *Phys.Rev.B*. 76, 11:115437.

Brach, R., Dunn, P., Li, X. (2000). Experiments and engineering models of microparticle impact and deposition. *J.Adhesion*. 74, 1-4:227-282.

Bradley, R. S. (1932). LXXIX. The cohesive force between solid surfaces and the surface energy of solids. *Philosophical Magazine Series 7*. 13, 86:853-862.

Cheng, Y., and Yeh, H. (1979). Particle bounce in cascade impactors. *Environ.Sci.Technol*. 13, 11:1392-1396.

Cheong, Y. S., Salman, A. D., Hounslow, M. J. (2003). Effect of impact angle and velocity on the fragment size distribution of glass spheres. *Powder Technol*. 138, 2–3:189-200.

Derjaguin, B., Muller, V., Toporov, Y. (1975). Effect of Contact Deformations on Adhesion of Particles. *J.Colloid Interface Sci*. 53, 2:314-326.

Dunbar, C., Kataya, A., Tiangbe, T. (2005). Reducing bounce effects in the Andersen cascade impactor. *Int.J.Pharm*. 301, 1–2:25-32.

Dunn, P., Brach, R., Caylor, M. (1995). Experiments on the Low-Velocity Impact of Microspheres with Planar Surfaces. *Aerosol Sci.Technol.* 23, 1:80-95.

Eggersdorfer, M. L., Kadau, D., Herrmann, H. J., Pratsinis, S. E. (2011). Multiparticle Sintering Dynamics: From Fractal-Like Aggregates to Compact Structures. *Langmuir*. 27, 10:6358-6367.

Ehara, K., Hagwood, C., Coakley, K. J. (1996). Novel method to classify aerosol particles according to their mass-to-charge ratio—Aerosol particle mass analyser. *J.Aerosol Sci.* 27, 2:217-234.

Feng, X., Li, H., Zhao, H., Yu, S. (2009). Numerical simulations of the normal impact of adhesive microparticles with a rigid substrate. *Powder Technol.* 189, 1:34-41.

Froeschke, S., Kohler, S., Weber, A., Kasper, G. (2003). Impact fragmentation of nanoparticle agglomerates. *J.Aerosol Sci.* 34, 3:275-287.

Guntay, S., Suckow, D., Dehbi, A., Kapulla, R. (2004). ARTIST: introduction and first results. Nucl.Eng.Des. 231, 1:109-120.

Jayadeep, U. B., Bobji, M. S., Jog, C. S. (2013). Energy Loss in the Impact of Elastic Spheres on a Rigid Half-Space in Presence of Adhesion. *Tribology Letters.*1-11.

John, W., and Sethi, V. (1993). Breakup of Latex Doublets by Impaction. *Aerosol Sci.Technol.* 19, 1:57-68.

Johnson, K.,L., Kendall, K., Roberts, A.,D. (1971). Surface Energy and the Contact of Elastic Solids. Proceedings of the Royal Society A: Mathematical, *Physical and Engineering Sciences.* 324, 1558:301-313.

Jung, S., Suh, D., Yoon, W. (2010). Molecular dynamics simulation on the energy exchanges and adhesion probability of a nano-sized particle colliding with a weakly attractive static surface. *J.Aerosol Sci.* 41, 8:745-759.

Kelly, W., and McMurry, P. (1992). Measurement of Particle Density by Inertial Classification of Differential Mobility Analyzer Generated Monodisperse Aerosols. *Aerosol.Sci.Technol.* 17, 3:199-212.

Kodas, T. and Hampton-Smith, M. (1999). Aerosol Processing of Materials. Wiley-VCH. p. 12, Fig. 1.8.

Konstandopoulos, A. (2006). Particle sticking/rebound criteria at oblique impact. *J.Aerosol Sci.* 37, 3:292-305.

Kusters, K. A., Pratsinis, S. E., Thoma, S. G., Smith, D. M. (1993). Ultrasonic fragmentation of agglomerate powders. *Chemical Engineering Science*. 48, 24:4119-4127.

Kwek, J. W., Heng, D., Lee, S. H., Ng, W. K., Chan, H. -., Adi, S., Heng, J., Tan, R. B. H. (2013). High speed imaging with electrostatic charge monitoring to track powder deagglomeration upon impact. *J.Aerosol Sci.* 65, 0:77-87.

Lähde, A., Kokkonen, N., Karttunen, A. J., Jääskelainen, S., Tapper, U., Pakkanen, T. A., Jokiniemi, J. (2011). Preparation of copper-silicon dioxide nanoparticles with chemical vapor synthesis. *J.Nanopart.Res*. 13, 9:3591-3598.

Lai, C., Huang, S., Chang, C., Lin, J. (2008). Reducing particle bounce and loading effect for a multi-hole impactor. *Aerosol Sci.Technol.* 42, 2:114-122.

Lechman, Jeremy. (2010). Aerosol Cluster Impact and Break-up: I. Model and Implementation. Vol. SAND2010-7105. Sandia National Laboratories.

Lechman, Jeremy, and Takoto, Yoichi. (2010). Aerosol Cluster Impact and Break-up: II. Atomic and Cluster Scale Models. Vol. SAND2010-6429. Sandia National Laboratories.

Li, X., Dunn, P. F., Brach, R. M. (2000). Experimental and numerical studies of microsphere oblique impact with planar surface. *J.Aerosol Sci.* 31, 5:583-594.

Li, X., Dunn, P. F., Brach, R. M. (1999). Experimental and numerical studies on the normal impact of microspheres with surfaces. *J.Aerosol Sci*. 30, 4:439-449.

Lind, T., Ammar, Y., Dehbi, A., Guentay, S. (2010). De-agglomeration mechanisms of TiO(2) aerosol agglomerates in PWR steam generator tube rupture conditions. *Nucl.Eng.Des.* 240, 8:2046-2053.

Liu, G., Li, S., Yao, Q. (2011). A JKR-based dynamic model for the impact of micro-particle with a flat surface. *Powder Technol.* 207, 1–3:215-223.

Liu, L., Kafui, K. D., Thornton, C. (2010). Impact breakage of spherical, cuboidal and cylindrical agglomerates. *Powder Technol.* 199, 2:189-196.

Lyyränen, J., Backman, U., Tapper, U., Auvinen, A., Jokiniemi, J. (2009). A size selective nanopartile collection device based on diffusion and thermophoresis. *J. Phys.:* Conference Series. 170, 012011:.

Lyyränen, J., Jokiniemi, J., Kauppinen, E., Backman, U., Vesala, H. (2004). Comparison of different dilution methods for measuring diesel particle emissions. *Aerosol Sci.Technol*. 38, 1:12-23.

Malloy, Q. G. J., Nakao, S., Qi, L., Austin, R., Stothers, C., Hagino, H., Cocker,David R.,,III. (2009). Real-Time Aerosol Density Determination Utilizing a Modified Scanning Mobility Particle SizerAerosol Particle Mass Analyzer System RID F-4442-2010. *Aerosol Sci.Technol.* 43, 7:673-678.

Mandelbrot, B. (1983). The fractal geometry of nature. *Earth Surf.Process.Landforms*. 8, 4:406-406.

Mandzy, N., Grulke, E., Druffel, T. (2005). Breakage of TiO_2 agglomerates in electrostatically stabilized aqueous dispersions. *Powder Technol.* 160, 2:121-126.

Marković, S., Mitrić, M., Starčević, G., Uskoković, D. (2008). Ultrasonic de-agglomeration of barium titanate powder. *Ultrason.Sonochem.* 15, 1:16-20.

Marple, VA. 1970. Fundamental study of inertial impactors. Ph.D. diss., Minnesota Univ., Minneapolis. Particle Technology Lab.

Marple, V., Rubow, K., Behm, S. (1991). A Microorifice Uniform Deposit Impactor (Moudi) - Description, Calibration, and use. *Aerosol Sci.Technol.* 14, 4:434-446.

McMurry, P. H., Wang, X., Park, K., Ehara, K. (2002). The Relationship between Mass and Mobility for Atmospheric Particles: A New Technique for Measuring Particle Density. *Aerosol Sci.Technol.* 36, 2:227-238.

Menter, F. R. (1994). Two-Equation Eddy-Viscosity Turbulence Models for Engineering Applications. *AIAA Journal.* 32, 8:1598-1605.

Miettinen, M., Riikonen, J., Tapper, U., Backman, U., Joutsensaari, J., Auvinen, A., Lehto, V. P., Jokiniemi, J. (2009). Development of a highly controlled gas-phase nanoparticle generator for inhalation exposure studies. *Hum.Exp.Toxicol.* 28, 6-7:413-419.

Mishra, B. K., and Thornton, C. (2001). Impact breakage of particle agglomerates. *Int.J.Miner.Process*. 61, 4:225-239.

Moreno, R., Ghadiri, M., Antony, S. J. (2003). Effect of the impact angle on the breakage of agglomerates: a numerical study using DEM. *Powder Technol.* 130, 1–3:132-137.

Moreno-Atanasio, R. (2012). Energy dissipation in agglomerates during normal impact. *Powder Technol.* 223, 0:12-18.

Pak, S. S., Liu, B. Y. H., Rubow, K. L. (1992). Effect of Coating Thickness on Particle Bounce in Inertial Impactors. *Aerosol Sci.Technol.* 16, 3:141-150.

Park, K., Cao, F., Kittelson, D., McMurry, P. (2003). Relationship between particle mass and mobility for diesel exhaust particles. *Environ.Sci.Technol.* 37, 3:577-583.

Qin, Z., and Pletcher, R. H. (2011). Particle impact theory including surface asperity deformation and recovery. *J.Aerosol Sci.* 42, 12:852-858.

Rennecke, S., and Weber, A. P. (2013). A novel model for the determination of nanoparticle impact velocity in low pressure impactors. *J.Aerosol Sci.* 55, 0:89-103.

Rennecke, S., and Weber, A. P. The critical velocity for nanoparticle rebound measured in a low pressure impactor. *J.Aerosol Sci.*0:.

Reuter-Hack, K., Weber, A. P., Roesler, S., Kasper, G. (2007). First LDA measurements of nanoparticle velocities in a low-pressure impacting jet. *Aerosol Sci.Technol.* 41, 3:277-283.

Reynolds, G. K., Fu, J. S., Cheong, Y. S., Hounslow, M. J., Salman, A. D. (2005). Breakage in granulation: A review. *Chemical Engineering Science.* 60, 14:3969-3992.

Rothenbacher, S., Messerer, A., Kasper, G. (2008). Fragmentation and bond strength of airborne diesel soot agglomerates. *Particle and Fibre Toxicology.* 5, 9.

Salman, A. D., Biggs, C. A., Fu, J., Angyal, I., Szabó, M., Hounslow, M. J. (2002). An experimental investigation of particle fragmentation using single particle impact studies. *Powder Technol.* 128, 1:36-46.

Seipenbusch, M., Froeschke, S., Weber, A., Kasper, G. (2002). Investigations on the fracturing of nanoparticle agglomerates - first results. *Proceedings of the Institution of Mechanical Engineers Part E-Journal of Process Mechanical Engineering.* 216, E4:219-225.

Seipenbusch, M., Rothenbacher, S., Kirchhoff, M., Schmid, H. -., Kasper, G., Weber, A. P. (2010). Interparticle forces in silica nanoparticle agglomerates. *J.Nanopart.Res.* 12, 6:2037-2044.

Seipenbusch, M., Toneva, P., Peukert, W., Weber, A. P. (2007). Impact fragmentation of metal nanoparticle agglomerates. *Particle & Particle Systems Characterization.* 24, 3:193-200.

Stronge, W. J., James, R., Ravani, B. (2001). Oblique impact with friction and tangential compliance. *Philosophical Transactions of the Royal Society of London.Series A: Mathematical, Physical and Engineering Sciences.* 359, 1789:2447-2465.

Teleki, A., Wengeler, R., Wengeler, L., Nirschl, H., Pratsinis, S. E. (2008). Distinguishing between aggregates and agglomerates of flame-made TiO_2 by high-pressure dispersion. *Powder Technol.* 181, 3:292-300.

Thornton, C., Ciomocos, M. T., Adams, M. J. (1999). Numerical simulations of agglomerate impact breakage. *Powder Technol.* 105, 1–3:74-82.

Thornton, C., and Yin, K. K. (1991). Impact of elastic spheres with and without adhesion. *Powder Technol.* 65, 1–3:153-166.

Thornton, C., Cummins, S. J., Cleary, P. W. (2013). An investigation of the comparative behaviour of alternative contact force models during inelastic collisions. *Powder Technol.* 233, 30-46.

Thornton, C., and Ning, Z. (1998). A theoretical model for the stick/bounce behaviour of adhesive, elastic-plastic spheres. *Powder Technol.* 99, 2:154-162.

Tong, Z. B., Yang, R. Y., Yu, A. B., Adi, S., Chan, H. K. (2009). Numerical modelling of the breakage of loose agglomerates of fine particles. *Powder Technol.* 196, 2:213-221.

Tsai, C., Pui, D., Liu, B. (1990). Capture and Rebound of Small Particles upon Impact with Solid-Surfaces. *Aerosol Sci.Technol.* 12, 3:497-507.

Virtanen, A., Joutsensaari, J., Koop, T., Kannosto, J., Yli-Pirila, P., Leskinen, J., Makela, J. M., Holopainen, J. K., Poeschl, U., Kulmala, M., Worsnop, D. R., Laaksonen, A. (2010). An amorphous solid state of biogenic secondary organic aerosol particles. *Nature*. 467, 7317:824-827.

Wall, S., John, W., Wang, H., Goren, S. L. (1990). Measurements of Kinetic Energy Loss for Particles Impacting Surfaces. *Aerosol Sci.Technol.* 12, 4:926-946.

Wang, H., and Kasper, G. (1991). Filtration Efficiency of Nanometer-Size Aerosol-Particles. *J.Aerosol Sci*. 22, 1:31-41.

Wang, S. C., and Flagan, R. C. (1990). Scanning Electrical Mobility Spectrometer. *Aerosol Sci.Technol.* 13, 2:230-240.

Weibull, W. (1951). A Statistical Distribution Function of Wide Applicability. *Journal of Applied Mechanics.* 293-297.

Weir, G., and McGavin, P. (2008). The coefficient of restitution for the idealized impact of a spherical, nano-scale particle on a rigid plane. *Proceedings of the Royal Society A-Mathematical Physical and Engineering Sciences.* 464, 2093:1295-1307.

Wengeler, R., and Nirschl, H. (2007). Turbulent hydrodynamic stress induced dispersion and fragmentation of nanoscale agglomerates. *J.Colloid Interface Sci.* 306, 2:262-273.

Wengeler, R., Teleki, A., Vetter, M., Pratsinis, S., Nirschl, H. (2006). High-pressure liquid dispersion and fragmentation of flame-made silica agglomerates. *Langmuir.* 22, 11:4928-4935.

Wittel, F. K., Carmona, H. A., Kun, F., Herrmann, H. J. (2008). Mechanisms in impact fragmentation. *Int.J.Fract.* 154, 1-2:105-117.

Wong, W., Fletcher, D. F., Traini, D., Chan, H., Crapper, J., Young, P. M. (2011). Particle aerosolisation and break-up in dry powder inhalers: Evaluation and modelling of impaction effects for agglomerated systems. *J.Pharm.Sci.* 100, 7:2744-2754.

Wu, C. Y., Thornton, C., Li, L. Y. (2003). Coefficients of restitution for elastoplastic oblique impacts. *Advanced Powder Techno.* 14, 4:435-448.

Wu, C., Thornton, C., Li, L. (2008). Rebound Behaviou of Spheres During Elastic-Plastic Oblique Impacts. *Int.J.Mod.Phys.*B. 22, 09:1095-1102.